

Enhancement of SSVEPs Classification in BCI-based Wearable Instrumentation Through Machine Learning Techniques

*Original*

Enhancement of SSVEPs Classification in BCI-based Wearable Instrumentation Through Machine Learning Techniques / Apicella, A.; Arpaia, P.; Benedetto, E. D.; Donato, N.; Duraccio, L.; Giugliano, S.; Prevete, R.. - In: IEEE SENSORS JOURNAL. - ISSN 1530-437X. - ELETTRONICO. - 22:9(2022), pp. 9087-9094. [10.1109/JSEN.2022.3161743]

*Availability:*

This version is available at: 11583/2962561 since: 2022-05-03T17:01:41Z

*Publisher:*

Institute of Electrical and Electronics Engineers Inc.

*Published*

DOI:10.1109/JSEN.2022.3161743

*Terms of use:*

This article is made available under terms and conditions as specified in the corresponding bibliographic description in the repository

*Publisher copyright*

IEEE postprint/Author's Accepted Manuscript

©2022 IEEE. Personal use of this material is permitted. Permission from IEEE must be obtained for all other uses, in any current or future media, including reprinting/republishing this material for advertising or promotional purposes, creating new collecting works, for resale or lists, or reuse of any copyrighted component of this work in other works.

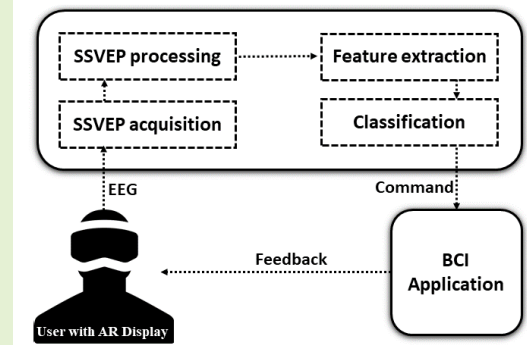
(Article begins on next page)

# Enhancement of SSVEPs Classification in BCI-based Wearable Instrumentation Through Machine Learning Techniques

Andrea Apicella, Pasquale Arpaia, *Senior Member, IEEE*, Egidio De Benedetto, *Senior Member, IEEE*, Nicola Donato, *Senior Member, IEEE*, Luigi Duraccio, Salvatore Giugliano, and Roberto Prevete

**Abstract**— This work addresses the adoption of Machine Learning classifiers and Convolutional Neural Networks to improve the performance of highly wearable, single-channel instrumentation for Brain-Computer Interfaces. The proposed measurement system is based on the classification of Steady-State Visually Evoked Potentials (SSVEPs). In particular, Head-Mounted Displays for Augmented Reality are used to generate and display the flickering stimuli for the SSVEPs elicitation. Four experiments were conducted by employing, in turn, a different Head-Mounted Display. For each experiment, two different algorithms were applied and compared with the state-of-the-art-techniques. Furthermore, the impact of different Augmented Reality technologies in the elicitation and classification of SSVEPs was also explored. The experimental metrological characterization demonstrates (i) that the proposed Machine Learning-based processing strategies provide a significant enhancement of the SSVEP classification accuracy with respect to the state of the art, and (ii) that choosing an adequate Head-Mounted Display is crucial to obtain acceptable performance. Finally, it is also shown that the adoption of inter-subjective validation strategies such as the Leave-One-Subject-Out Cross Validation successfully leads to an increase in the inter-individual  $1-\sigma$  reproducibility: this, in turn, anticipates an easier development of ready-to-use systems.

**Index Terms**— Augmented Reality, Brain-Computer Interface, BCI, EEG, Industry 4.0, Instrumentation, Machine Learning, Neural Networks, SSVEP, Real-Time Systems, Wearable.



## I. INTRODUCTION

Brain-Computer Interfaces (BCIs) are an emerging technology able to create a direct communication path between the human brain and external devices, without the use of peripheral nerves and muscles [1]–[4]. Among the major BCI paradigms, Steady-State Visually Evoked Potential (SSVEP) has rapidly gained interest for developing applications in several fields, such as rehabilitation [5], [6], gaming [7],

This work was carried out as part of the “ICT for Health” project, which was financially supported by the Italian Ministry of Education, University and Research (MIUR), under the initiative ‘Departments of Excellence’ (Italian Budget Law no. 232/2016), through an excellence grant awarded to the Department of Information Technology and Electrical Engineering of the University of Naples Federico II, Italy.

A. Apicella, E. De Benedetto, S. Giugliano and R. Prevete are with the Department of Electrical Engineering and Information Technology, University of Naples Federico II, Naples, 80125 Italy (e-mail: egidio.debenedetto@unina.it).

P. Arpaia is with the Interdepartmental Research Center in Health Management and Innovation in Healthcare, University of Naples Federico II, Naples, 80125 Italy (e-mail: pasquale.arpaia@unina.it).

N. Donato is with the Department of Engineering, University of Messina, Messina, 98122, Italy (e-mail: nicola.donato@unime.it).

L. Duraccio is with the Department of Electronics and Telecommunications, Polytechnic University of Turin, Turin, 10129, Italy (e-mail: luigi.duraccio@polito.it).

entertainment [8], industrial inspection [9], [10], and health monitoring [11], since it is characterized by easier detection and higher Information Transfer Rates (ITRs) with respect to other available BCIs [12], [13].

In particular, SSVEPs are a specific physiological brain response to continuously flickering visual stimuli, typically induced after a latency varying from 80 ms to 160 ms [14]. Stimulation frequency bands usually range from 6 Hz to 30 Hz, although the best Signal to Noise Ratio (SNR) is achieved in the range 8-15 Hz [15]. Generally, the SSVEP shows a sinusoidal-like waveform, with a fundamental frequency equal to that of the gazed stimulus, and often higher harmonics [16], as shown in Fig. 1. In practical applications, different visual stimuli (at different frequencies) are associated to specific commands: thus, such systems allow the user to perform a selection by simply looking at the related flickering stimulus. In traditional SSVEP-based experimental setups, the SSVEPs are acquired through a multi-channel electroencephalogram (EEG) data acquisition [17], while the flickering stimuli are often visualized on a LCD monitor. However, this benchtop instrumentation limits the portability of the system, thus confining the use of BCI-SSVEP to laboratory environments. Recently, wearable solutions, based on single-channel acqui-

sitions, have been proposed in the literature [18], [19]. Additionally, the use of Augmented Reality (AR) Head-Mounted Displays (HMDs), which are emerging devices of the 4.0 scenario [20], is establishing itself as a promising strategy to render the flickering stimuli and guarantee, at the same time, more immersivity and engagement in the fruition of BCI applications [21]–[23].

Nevertheless, the overall performance of combined AR-BCI instruments strongly depends on the specifications of the HMD; in particular, on two characteristics. First, the field of view (FOV) of HMDs is generally limited to some tens of degrees: this limits the maximum number of flickering stimuli that can be rendered simultaneously on the HMD. At the state of the art, good performance has been achieved when, at most, two visual stimuli are simultaneously displayed [6]. Secondly, AR HMDs exhibit a significant non-predictability of the frame rate. This uncertainty leads to a shift in the frequency values of the rendered stimuli, thus reducing the classification accuracy of the SSVEP elicited on the user's EEG [11].

To preserve wearability of SSVEP-based AR-BCI instrumentation, while still ensuring optimal performance, the challenge is to keep the results obtained using HMDs close to those achieved through traditional setups [24]. At the state of art, algorithms based on the Canonical Correlation Analysis (CCA) provide the best performance in terms both of classification accuracy and time response [24], [25]. Another promising strategy is the adoption of Machine Learning (ML) techniques [26], in particular: (i) classical ML classifiers, such as Support Vector Machine (SVM), k-Nearest Neighbors (k-NN) [27], [28], and (ii) Artificial and Convolutional Neural Networks (ANN, CNN) [29], [30]. In fact, recent works [30]–[32] showed that, for low-channel EEG setups, these strategies allow to outperform the results obtained through CCA. For example, in [30] a one-dimensional CNN was realized for a single-channel BCI instrument, managing to classify five-class SSVEPs with an accuracy of 99% at 4-s time response (whereas CCA reached 91% in the same conditions). A multi-dimensional CNN, called *PodNet*, was proposed in [31] for a three-channel setup: this CNN exceeded the results obtained by CCA by about 5% at 2-s time response. Therefore, in a single-channel AR-based instrumentation, the adoption of traditional Machine Learning classifiers and Neural Networks can represent an effective alternative to CCA.

Based on these considerations, in this paper, a metrological characterization of a highly-wearable, AR-based SSVEP BCI is performed. The aim is twofold: first, evaluating the classification performance by comparing the adoption of the aforementioned classifiers (SVM, k-NN, ANN, CNN) with the state-of-the-art CCA; to this purpose, two algorithms were designed, implemented and comparatively tested after four different experiments. Each experiment was characterized by the use of a different AR HMD to generate the flickering stimuli. In this way, also a comparison between the impact of different AR technologies in the elicitation of SSVEPs was conducted.

The paper is organized as follows. Section II describes the proposal in detail. The experimental metrological characterization is reported and discussed in Section III, while the

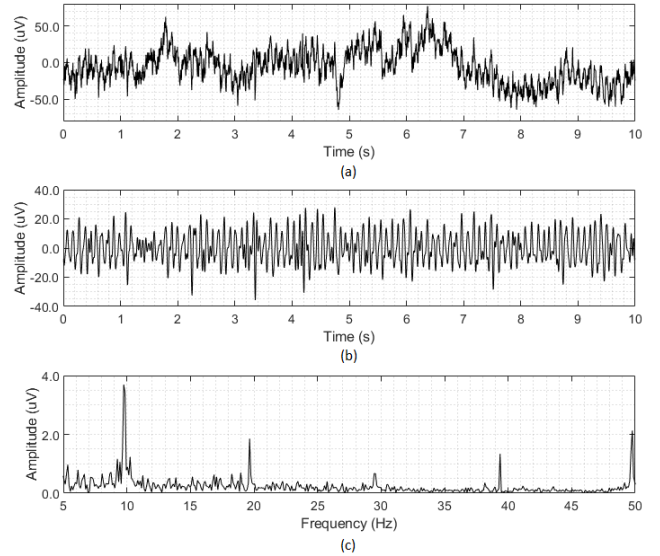


Fig. 1. Example of a SSVEP of a user staring at a 10 Hz-flickering stimulus: EEG in the time domain (a); Filtered EEG in the time domain (b); EEG in the frequency domain (c).

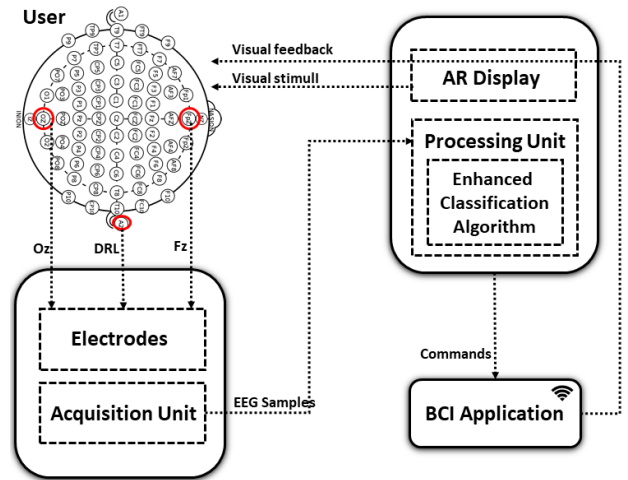


Fig. 2. Architecture of the wearable BCI-SSVEP system used for testing the proposed algorithm.

obtained results are shown in Section IV. Finally, in Section V, conclusions are drawn.

## II. PROPOSAL

In this work, an enhancement of the SSVEP classification performance for highly wearable BCI instrumentation is proposed. To this aim, the architecture of the single-channel BCI developed in [6], [9], [11] was considered. This measurement system is based on the real-time classification of users SSVEPs elicited by AR HMDs. Such instrumentation is particularly challenging for wearable applications as the number of electrodes is very limited.

Fig. 2 summarizes the major blocks of the system architecture. In particular, an *AR Display* renders the flickering stimuli

in the range 8-15 Hz for the SSVEPs elicitation. Then, only three *Electrodes* are used: a pair of active and dry [33] electrodes are placed in *Oz*, *Fz* positions according to the 10-20 International System [6] to capture the user EEG signal; while a passive electrode (*Driven Right Leg*, *DRL*) is placed on the earlobe and acts as a reference. In this way, a single-channel, differential configuration is implemented, reducing the common mode interference. The brain signal is digitized by a portable *Acquisition Unit*, which sends the EEG Samples to a portable *Processing Unit*. The signal is processed by adopting an *Enhanced Classification Algorithm*, and the detected command is sent in real time to the *BCI Application*, which actuates the received command and also provides a visual feedback to the User to show the output of the desired selection.

In this work, two strategies were pursued to for enhancing the classification algorithm block:

- 1) Feature Reduction (FR); and
- 2) Deep SSVEP Convolutional Unit (SCU).

In the following sections, both strategies are presented and discussed in detail.

### A. Features Reduction (FR)

The main blocks of FR algorithm, which was fully designed and implemented by the Authors, are shown in Fig. 3(a). As visible, the *EEG Samples* are processed both in frequency and time domains, in order to obtain a reduced number of significant features.

- In the frequency domain, first, a single-sided amplitude spectrum is obtained by means of a Fast Fourier Transform (FFT). No windowing is applied to the original samples. Then, the actual SSVEPs *Peaks* are detected around the  $n$  rendered stimulus frequencies: given a generic nominal frequency value  $f_n$ , the interval  $[f_n \cdot 0.9, f_n \cdot 1.1]$  was used to find the actual peak frequency  $f_a$ . This interval was considered suitable in order to properly mitigate the uncertainty introduced by the fps variations of the AR HMDs in the rendering of the flickering stimuli. Consequently, the resulting Power Spectral Density (PSDs) coefficients [9] are more accurate.
- In the time domain, first, a *Band pass Filtering* between 5 and 25 Hz is applied by means of a Finite Impulsive Response (FIR) filter with linear phase response. Then, the *Canonical Correlation Analysis* between the filtered signal and a set of sinewaves, having the frequencies of the  $n$  detected peaks and variable phase [6], is performed. In this way, also the  $n$  canonical correlation coefficients obtained for each frequency are more accurate.

Ultimately, for a given brain signal composed of a number  $f_s \cdot N$  of EEG samples and  $n$  classes (where  $f_s$  is the sampling frequency,  $N$  is the number of seconds, and  $n$  is the number of stimulus frequencies), only  $2n$  features are extracted and normalized. Finally, the *Classification* is carried out with three ML classifiers: in particular, Support Vector Machine (SVM), k-Nearest Neighbor (k-NN), and Artificial Neural Network (ANN) are employed since they guarantee the best results with acceptable computational effort [27]–[29].

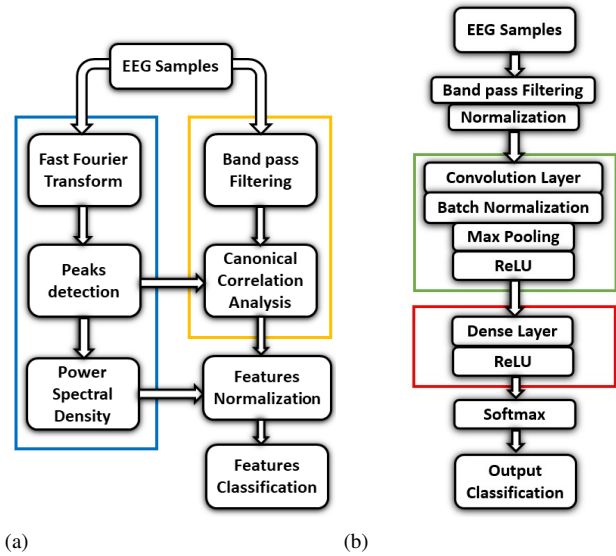


Fig. 3. Block diagram of the Features Reduction (a) and DeepSCU (b) classification algorithms. For the Feature Reduction architecture, the two boxes represent a processing conducted in frequency (blue box) and time (yellow box) domain. For the DeepSCU architecture, the SCU and Dense blocks are highlighted in green and red, respectively.

- SVM is a binary classifier which separates data through a decision hyperplane. SVM considers the inputs as points in a vector space, finding an optimal hyperplane in order to maximize the distance from the class boundaries.
- k-NN is a non-parametric ML method. It can be described as follows: given a set of already labeled points, a positive integer  $k$ , and a distance measure  $d$  (e.g., Euclidean), for a new input point  $p$ , k-NN labels  $p$  as the most present class among its  $k$  neighbors (through the measure  $d$ ) that are in the labelled set.
- ANN is a Feed-Forward Artificial Neural Network where there are one or more layers of hidden neurons between the input and output layers. Each layer has weighted connections ( $W$ ) entering from the previous layer and outgoing in the next one, so the propagation of the signal occurs forward without loops and without cross connections. In the learning phase, a error function  $E(W)$  is minimized through a proper learning algorithm as Gradient Descent.

### B. Deep SSVEP Convolutional Unit (SCU)

In Aznan et Al. [34], the Deep SCU neural network architecture was proposed, showing promising results in classification tasks using SSVEP signals as input. Differently from the *FR* algorithm, this processing strategy adopts all the EEG samples acquired in the time window. It consists of one or more neural network layers blocks (defined *SCU blocks*). Each SCU block is composed of the following layers:

- *1D Convolutional layer*: a 1D convolution is performed on the EEG samples. The time window (kernel) scrolls along one dimension, returning a feature maps on the basis of the number of filters chosen.
- *Batch Normalization layer*: a transformation is applied in

TABLE I  
CLASSIFIERS, OPTIMIZED HYPERPARAMETERS, AND VARIATION RANGES

Classifier	Optimized Hyperparameter	Variation Range
<b>k-Nearest Neighbour (k-NN)</b> <sup>1</sup>	Distance	{Minkowski, Chebychev, Manhattan, Cosine, Euclidean}
	Distance Weight	{equal, inverse, squaredinverse}
	Num Neighbors	{3, 5, 6, 7}
<b>Support Vector Machine (SVM)</b> <sup>1</sup>	C Regularization	{0.01, 0.10, 1.00, 1.77, 5.00, 10.00, 15.00}
	Kernel Function	{linear, radial basis, polynomial}
	Polynomial Order	{2, 3, 4}
<b>Artificial Neural Network (ANN)</b> <sup>1</sup>	Activation Function	{relu, tanh}
	Hidden Layer nr. of Neurons	[5, 505] step: 50
	Learning Rate	{0.0005, 0.0001, 0.0010, 0.0050, 0.0100}
	Validation Fraction	{0.2, 0.3}
<b>Deep SSVEP Convolutional Unit</b> <sup>2</sup>	Convolutional Layer nr. of Filters	[16, 1024] step: x2
	SCU Blocks	[1, 7] step: 1
	Kernel Size	{10, 20, 30}
	Dense Layer nr. of Neurons	[60, 1260] step: 200
	Dense Blocks	{1, 2}
	Learning Rate	{0.0001, 0.0010}
	Validation Fraction	{0.2, 0.3}

<sup>1</sup>FR Algorithm

<sup>2</sup>Deep SCU Algorithm

order to keep the average and the standard deviation of the output close to 0 and 1, respectively.

- *Max Pooling layer*: it downsamples the input representation of the previous layer by taking the maximum value on a spatial window of size equal to 2.
- *Rectifier Linear Unit (ReLU)* activation function: it is applied at the end of each SCU block. It is a function that returns 0 if it receives negative input, otherwise it returns the received value, thus increasing the sparsity in the output.

Finally, fully-connected (Dense) layers equipped with *ReLU* activation functions are used as final layers of the network. The optimal number of SCU blocks, Dense blocks, and the optimal values of the hyper parameters are found through a grid-search approach (see Table I for the parameters ranges used in the experiments). In the grid search, the number of SCU blocks varies from a minimum of 1 to a maximum of 7. In each sequential SCU block, convolutional layers with a variable number of filters are considered. For the sake of the example, with 7 SCU blocks the number of filters for each convolutional layer is the following: [16, 32, 64, 128, 256, 512, 1024]. Similarly, for Dense blocks, in which 1 or maximum 2 blocks were different combinations in the number of neurons between the different dense (fully-connected) layers are considered.

In Fig. 3(b) an example of SCU architecture with one SCU block and one full-connected layer is shown. With respect to the approach proposed in [34], the Deep SCU architecture is now applied to a single-channel setup. Furthermore, the *EEG Samples* are pre-processed by a *FIR Band pass filter* between 5 and 25 Hz with linear phase response, and then normalized.

### III. EXPERIMENTAL METROLOGICAL CHARACTERIZATION

A metrological characterization of the proposed algorithm was performed by conducting four experiments involving healthy adult volunteers. For each campaign, a different AR

HDM (which acted as the *AR Display* shown in Fig. 2) was adopted. These devices were used to elicit the users' SSVEPs in the range 8-15 Hz. Consequently, four distinct data sets for the testing of the SSVEPs classification algorithms were provided (one for each HMD).

#### A. Hardware and software

The AR devices used in this work are listed below:

- *Epson Moverio BT-200*: Moverio BT-200 are AR Smart Glasses with a 60 Hz Refresh Rate and a 23° diagonal FOV. They are equipped with Android 4.0.
- *Epson Moverio BT-350*: Like BT-200 version, Moverio BT-350 have a 23° diagonal FOV; however, the refresh rate is limited to 30 Hz and the operative system on board is Android 5.1.
- *Microsoft HoloLens 1*: Microsoft HoloLens 1 is an Optical-See-Through (OST) AR HMD with a 60 Hz Refresh Rate and a diagonal FOV of 34°.
- *Oculus Rift S*: Oculus Rift S is a HMD with 80 Hz Refresh Rate. It is originally designed for Virtual Reality. Thus, the integration of a HD Stereoscopic Camera (*Zed Mini*) allows to use the device as a Video-See-Through (VST) AR HMD.

The software employed to realize the AR environment for the selected HMDs are described as follows.

- *Epson Moverio BT-200/350*: the AR applications running on the Moverio glasses was developed in Android Studio. In particular, the flickering squares were generated by means the the Android library OpenGL.
- *Microsoft HoloLens and Oculus Rift S*: the AR environment for HoloLens and Oculus Rift was developed in Unity 3D.

In all these cases, the flickering frequencies were realized with a suitable white/black pixels alternation. For instance, given a refresh rate of 60 Hz, a 10-Hz frequency is generated with a

TABLE II  
DETAILS OF THE DATA SETS

Data Set Index	#1	#2	#3	#4
AR Device	BT-200	BT-350	Hololens	Rift S
Volunteers	20	9	9	9
Classes	2	4	4	4
Signals/subject	24	20	20	20
Signal length (s)	10	10	10	10

white/black alternation each three frame [35], while not sub-multiple frequency values are obtained as a rounded average of a variable frequency stimulus [36].

The wearable Acquisition Unit chosen to acquire the users' brain signals is the Olimex EEG-SMT, a 10-bit, 256 S/s, open-source Analog-to-Digital converter. It was preferred to other consumer-grade EEG equipment such as *Emotiv Epoch* or *Neurosky Mindwave* [37]–[39] since: (i) a recent metrological characterization confirmed its suitability for BCI applications [40], as it showed strong linearity and no long-term drift; (ii) it has a very low cost (approximately 100 \$). Finally, the digitized signal is processed by a Raspberry Pi 4, a portable single-board PC.

### B. Data sets descriptions and validation strategy

Four different data sets were obtained by using each of the considered four AR devices. The two algorithms were validated on each data set by means of Leave One Subject Out Cross Validation (LOSO CV). This represents a promising inter-individual validation approach aimed at increasing reproducibility [41]. A grid search for the tuning of the models hyperparameters was adopted. In Table I, the hyperparameters values are reported for each classifier model.

Furthermore, in Table II the experimental details, regarding the four AR devices, and the number of volunteers, classes, and signals acquired for each subject, are provided. The number of classes indicate the number of simultaneous flickering stimuli rendered by the AR Device. As visible, the processing of the data set #1 is a binary classification problem, since only two frequencies are used. Instead, data sets #2, #3, and #4 are characterized by the adoption of four frequencies. In particular, the frequencies chosen for each data set are listed below:

- Data set #1 (BT-200): [10.00, 12.00] Hz
- Data set #2 (BT-350): [8.00, 10.00, 12.00, 15.00] Hz
- Data set #3 (Hololens): [8.57, 10.00, 12.00, 15.00] Hz
- Data set #4 (Rift S): [8.00, 10.00, 11.43, 13.33] Hz

The rendered stimuli are placed at the edges of the display to avoid interferences. For each trial, each volunteer was asked to focus at the selected stimulus for 10 s.

The performance of the proposed method was assessed both on the accuracy and the related time response: the time response is the signal duration  $T$  (also called epoch) extracted for each trial and then classified; on the other hand, the classification accuracy is the percentage of data set correctly classified.

## IV. RESULTS

Table III summarizes the results obtained through the proposed algorithms, compared with those achieved through

TABLE III  
CLASSIFICATION ACCURACY AND CORRESPONDING  $1-\sigma$  REPRODUCIBILITY ON THE FOUR DATA SETS

Data set #1 (Moverio BT-200)			
T (s)	CCA [6] (%)	Deep SCU (%)	FR* (%)
0.5	70.8 ± 10.0	74.4 ± 9.5	<b>75.0 ± 9.5</b>
1.0	74.8 ± 18.1	81.6 ± 9.6	<b>82.1 ± 9.8</b>
2.0	84.9 ± 12.1	87.5 ± 8.0	<b>89.2 ± 7.8</b>
3.0	91.0 ± 9.4	91.9 ± 7.3	<b>93.7 ± 5.6</b>
5.0	95.4 ± 5.6	95.7 ± 4.9	<b>96.7 ± 3.9</b>
10.0	-	97.7 ± 4.5	<b>99.4 ± 2.7</b>
Data set #2 (Moverio BT-350)			
T (s)	CCA [6] (%)	Deep SCU (%)	FR* (%)
0.5	-	30.9 ± 7.1	<b>39.2 ± 13.5</b>
1.0	-	35.8 ± 10.4	<b>46.3 ± 19.2</b>
2.0	51.9 ± 27.0	42.8 ± 13.2	<b>53.9 ± 23.5</b>
3.0	53.3 ± 25.6	43.5 ± 21.1	<b>56.7 ± 24.9</b>
5.0	56.7 ± 23.9	41.4 ± 17.9	<b>57.5 ± 23.7</b>
10.0	-	47.2 ± 23.0	<b>62.2 ± 24.5</b>
Data set #3 (Hololens)			
T (s)	CCA [6] (%)	Deep SCU (%)	FR* (%)
0.5	-	<b>48.4 ± 11.3</b>	44.9 ± 10.0
1.0	-	56.9 ± 13.9	<b>66.8 ± 16.7</b>
2.0	58.9 ± 20.6	72.3 ± 14.4	<b>76.4 ± 16.9</b>
3.0	70.5 ± 18.5	77.0 ± 15.8	<b>82.6 ± 13.1</b>
5.0	72.9 ± 28.3	80.0 ± 13.8	<b>88.9 ± 8.6</b>
10.0	-	75.0 ± 19.3	<b>94.4 ± 8.3</b>
Data set #4 (Oculus Rift S)			
T (s)	CCA [6] (%)	Deep SCU (%)	FR* (%)
0.5	-	36.7 ± 10.5	<b>42.7 ± 16.8</b>
1.0	-	40.6 ± 16.2	<b>54.0 ± 21.5</b>
2.0	56.1 ± 24.2	46.4 ± 18.6	<b>62.3 ± 23.5</b>
3.0	64.8 ± 20.9	56.3 ± 20.6	<b>65.7 ± 25.3</b>
5.0	68.5 ± 23.2	55.3 ± 18.6	<b>70.6 ± 23.8</b>
10.0	-	48.9 ± 21.2	<b>72.2 ± 23.3</b>

\*Only the best result is reported for brevity.

the CCA used in [6]. It can be seen that the enhancement reached by the FR algorithm is significant on each data set. The main contribution to this improvement is given by the peak detection block, which allows to obtain more accurate features both in time and frequency domains, thus mitigating the uncertainty caused by unpredictable fps variation of AR devices. For the sake of example, Fig. 4 (top) shows the fps variation of Epson Moverio BT-350. Despite the declared 30 Hz refresh rate, the average fps obtained are approximately 32. This translates into a shift of the rendered frequencies, as visible in the bottom image of Fig. 4. In this case, a white/black pixel alternation [35] generates a 16 Hz stimulus, instead of the expected 15 Hz. Thus, an adaptive strategy to find the FFT peak position represents the best solution to improve the SSVEP classification, especially in AR-based setup. On the other hand, Deep SCU algorithm outperforms CCA only on data sets #1 and #3. However, in all the data sets, the CCA strategy is characterized by a worse inter-individual  $1-\sigma$  reproducibility. Thus, the model built by CCA offers lower possibility to be generalized.

With regards to the comparison between the performance of each AR HMD, it is visible that Epson Moverio BT-200 (data set #1) provides the best classification accuracy (almost 90% at 2 s). The main reason is that only two flickering

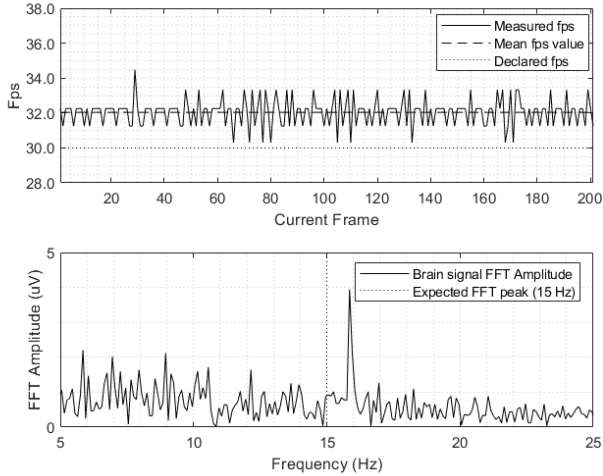


Fig. 4. Epson Moverio BT-350: measured and expected fps (top); measured and expected FFT peak of the relative user brain signal (bottom)

stimuli were rendered simultaneously on the display. When considering the four-stimuli data sets (i.e., data set #2, #3, and #4) the performance are significantly worse. In fact, Microsoft Hololens 1 (data set #3) reaches a classification accuracy of about 76% at 2 s, while Epson Moverio BT-350 (data set #2) and Oculus Rift S (data set #4) achieve about 54% and 62%, respectively. Clearly, the larger field of view of Microsoft Hololens 1 (with respect to Epson Moverio BT-350), and its Optical See-Through technology (with respect to Oculus Rift) contribute to this difference in the outcomes. Overall, it is evident the need of an adequate field of view when the number of concurrent flickering stimuli increases, in order to avoid interferences when users stare at the desired icon.

An overview of the results obtained through the FR algorithm on data set #1 is provided in Fig. 5 and Table IV. In particular, Fig. 5 shows the scatter plots of the features extracted by the FR algorithm. As visible, even with 1-s epochs, it is possible to discriminate the two classes. Clearly, increasing the duration of the epochs leads to an easier patterns separation and, thus, to an increase of the classification accuracy. Finally, Table IV provides a focus on the obtained results for each model used. The best performance are obtained by ANN classifier; however, even a more simple classifier like k-NN reaches comparable accuracy levels.

## V. CONCLUSIONS

This work proposes the adoption of ML techniques to enhance the classification performance of a highly wearable, single-channel instrumentation for BCI, based on the detection and classification of SSVEPs. In this measurement system, AR HMDs are used to generate the flickering stimuli necessary to SSVEPs elicitation; it guarantees greater immersivity and engagement with respect to traditional LCDs.

Two different ML-based algorithms were implemented to improve the SSVEP classification, in terms of classification accuracy and time response. Experimental results on four exper-

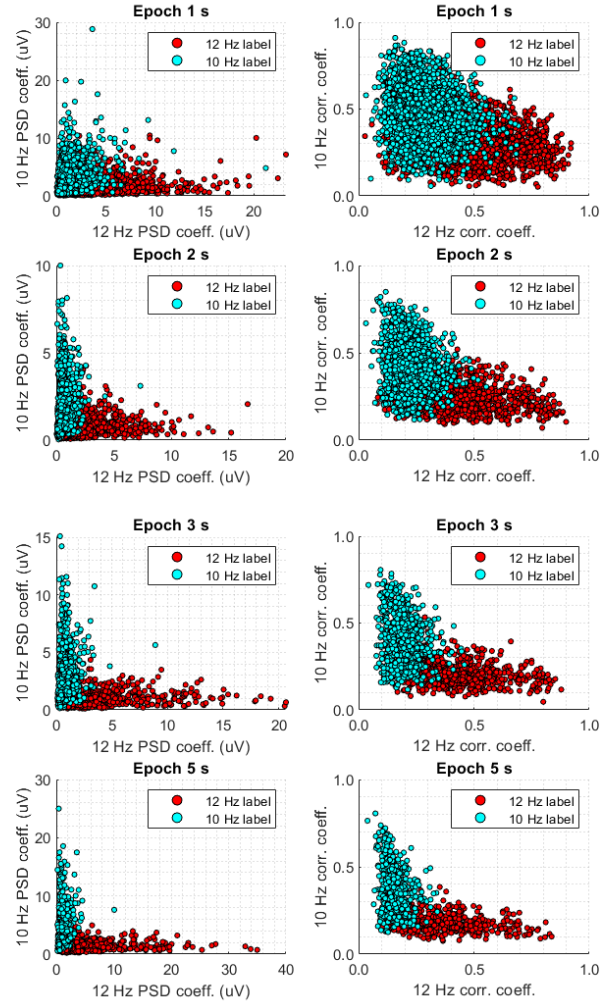


Fig. 5. Scatter plots of the extracted features for data set #1 (BT-200) with different time responses (epochs).

TABLE IV  
FR ALGORITHM RESULTS OBTAINED FOR DATA SET #1 (BT-200) FOR EACH CONSIDERED MODEL

T (s)	k-NN (%)	SVM (%)	ANN (%)
0.5	72.8 ± 9.3	74.8 ± 9.6	<b>75.0 ± 9.5</b>
1.0	80.7 ± 9.8	82.0 ± 9.8	<b>82.1 ± 9.8</b>
2.0	88.3 ± 8.8	<b>89.2 ± 7.8</b>	<b>89.2 ± 7.8</b>
3.0	93.3 ± 5.9	93.6 ± 5.2	<b>93.7 ± 5.6</b>
5.0	96.4 ± 4.8	96.4 ± 4.7	<b>96.7 ± 3.9</b>
10.0	99.0 ± 2.9	99.2 ± 2.8	<b>99.4 ± 2.7</b>

iments showed a significant enhancement of the performance with respect to the consolidated CCA-based algorithm. In particular, the combined use of both time-domain and frequency-domain features helps to mitigate the uncertainty introduced by AR devices regarding the generation of the visual stimuli. This translates into a better discrimination between classes and, thus, into an improvement of the system performance, without a significant increase of computational complexity. In fact, the obtained results also demonstrate that even a simple classifier like k-NN can outperform traditional processing strategies such as CCA. This represents a great advantage

in the development of wearable devices, when a low number of channel is used and a small computational complexity is required. An additional advantage in using ML is the increase in the inter-individual  $1-\sigma$  reproducibility, which leads to more “ready-to-use” systems. Finally, the experimental results show a significant difference in the classification accuracy between two-stimuli and four-stimuli setups. In fact, it was observed that increasing the number of concurrent stimuli inevitably led to a decrease of the classification accuracy (more than 20%). This is due to the reduced field of view of the devices which causes interference between gazed and not-gazed flickering stimuli. Further works will be dedicated to research a strategy to increase the number of concurrent AR-based flickering stimuli, still keeping the state-of-the-art performance, in order to ensure high performance for a practical use in daily life.

## REFERENCES

- [1] P. K. Shukla, R. K. Chaurasiya, S. Verma, and G. R. Sinha, “A thresholding-free state detection approach for home appliance control using p300-based bci,” *IEEE Sensors Journal*, vol. 21, no. 15, pp. 16927–16936, 2021.
- [2] S. Chaudhary, S. Taran, V. Bajaj, and A. Sengur, “Convolutional neural network based approach towards motor imagery tasks eeg signals classification,” *IEEE Sensors Journal*, vol. 19, no. 12, pp. 4494–4500, 2019.
- [3] B.-S. Lin, H.-A. Wang, Y.-K. Huang, Y.-L. Wang, and B.-S. Lin, “Design of ssvep enhancement-based brain computer interface,” *IEEE Sensors Journal*, vol. 21, no. 13, pp. 14330–14338, 2021.
- [4] P. Autthasan, X. Du, J. Arnin, S. Lamyai, M. Perera, S. Ithipuripat, T. Yagi, P. Manoonpong, and T. Wilaiprasitporn, “A single-channel consumer-grade eeg device for brain–computer interface: Enhancing detection of ssvep and its amplitude modulation,” *IEEE Sensors Journal*, vol. 20, no. 6, pp. 3366–3378, 2020.
- [5] X. Zhao, Y. Chu, J. Han, and Z. Zhang, “SSVEP-based brain–computer interface controlled functional electrical stimulation system for upper extremity rehabilitation,” *IEEE Transactions on Systems, Man, and Cybernetics: Systems*, vol. 46, no. 7, pp. 947–956, 2016.
- [6] P. Arpaia, L. Duraccio, N. Moccaldi, and S. Rossi, “Wearable brain–computer interface instrumentation for robot-based rehabilitation by augmented reality,” *IEEE Transactions on Instrumentation and Measurement*, vol. 69, no. 9, pp. 6362–6371, 2020.
- [7] I. Martišius and R. Damaševičius, “A prototype SSVEP based real time BCI gaming system,” *Computational intelligence and neuroscience*, vol. 2016, 2016.
- [8] C.-M. Wu, Y.-J. Chen, I. A. Zaeni, and S.-C. Chen, “A new SSVEP based BCI application on the mobile robot in a maze game,” in *2016 International Conference on Advanced Materials for Science and Engineering (ICAMSE)*, pp. 550–553, IEEE, 2016.
- [9] L. Angrisani, P. Arpaia, A. Esposito, and N. Moccaldi, “A wearable brain–computer interface instrument for augmented reality-based inspection in industry 4.0,” *IEEE Transactions on Instrumentation and Measurement*, vol. 69, no. 4, pp. 1530–1539, 2019.
- [10] Y. Li and T. Kesavadas, “SSVEP-based brain-computer interface for part-picking robotic co-worker,” *Journal of Computing and Information Science in Engineering*, vol. 22, no. 2, p. 021001, 2021.
- [11] P. Arpaia, E. De Benedetto, and L. Duraccio, “Design, implementation, and metrological characterization of a wearable, integrated AR-BCI hands-free system for health 4.0 monitoring,” *Measurement*, vol. 177, p. 109280, 2021.
- [12] R. Abiri, S. Borhani, E. W. Sellers, Y. Jiang, and X. Zhao, “A comprehensive review of eeg-based brain–computer interface paradigms,” *Journal of neural engineering*, vol. 16, no. 1, p. 011001, 2019.
- [13] Y. Zhang, S. Q. Xie, H. Wang, and Z. Zhang, “Data analytics in steady-state visual evoked potential-based brain–computer interface: A review,” *IEEE Sensors Journal*, vol. 21, no. 2, pp. 1124–1138, 2021.
- [14] C. Jia, X. Gao, B. Hong, and S. Gao, “Frequency and phase mixed coding in SSVEP-based brain–computer interface,” *IEEE Transactions on Biomedical Engineering*, vol. 58, no. 1, pp. 200–206, 2010.
- [15] Y. Wang, R. Wang, X. Gao, B. Hong, and S. Gao, “A practical vep-based brain-computer interface,” *IEEE Transactions on neural systems and rehabilitation engineering*, vol. 14, no. 2, pp. 234–240, 2006.
- [16] G. R. Müller-Putz, R. Scherer, C. Brauneis, and G. Pfurtscheller, “Steady-state visual evoked potential (SSVEP)-based communication: impact of harmonic frequency components,” *Journal of neural engineering*, vol. 2, no. 4, p. 123, 2005.
- [17] E. Yin, Z. Zhou, J. Jiang, Y. Yu, and D. Hu, “A dynamically optimized SSVEP brain–computer interface (BCI) speller,” *IEEE Transactions on Biomedical Engineering*, vol. 62, no. 6, pp. 1447–1456, 2014.
- [18] L.-W. Ko, S. Ranga, O. Komarov, and C.-C. Chen, “Development of single-channel hybrid BCI system using motor imagery and ssvep,” *Journal of healthcare engineering*, vol. 2017, 2017.
- [19] P. Arpaia, N. Moccaldi, R. Prevete, I. Sannino, and A. Tedesco, “A wearable EEG instrument for real-time frontal asymmetry monitoring in worker stress analysis,” *IEEE Transactions on Instrumentation and Measurement*, vol. 69, no. 10, pp. 8335–8343, 2020.
- [20] P. Arpaia, E. De Benedetto, C. A. Dodaro, L. Duraccio, and G. Servillo, “Metrology-based design of a wearable augmented reality system for monitoring patient’s vitals in real time,” *IEEE Sensors Journal*, vol. 21, no. 9, pp. 11176–11183, 2021.
- [21] Y. Ke, P. Liu, X. An, X. Song, and D. Ming, “An online SSVEP-BCI system in an optical see-through augmented reality environment,” *Journal of neural engineering*, vol. 17, no. 1, p. 016066, 2020.
- [22] A. Tedesco, D. Dallet, and P. Arpaia, “Augmented reality (AR) and brain-computer interface (BCI): Two enabling technologies for empowering the fruition of sensor data in the 4.0 era,” in *Proceedings of the AISEM 2020 Regional Workshop*, vol. 753, pp. 85–91, 2021.
- [23] P. Arpaia, E. De Benedetto, L. De Paolis, G. D’Errico, N. Donato, and L. Duraccio, “Highly wearable SSVEP-based BCI: Performance comparison of augmented reality solutions for the flickering stimuli rendering,” *Measurement: Sensors*, vol. 18, p. 100305, 2021.
- [24] Y. Wang, X. Chen, X. Gao, and S. Gao, “A benchmark dataset for SSVEP-based brain–computer interfaces,” *IEEE Trans. Neural Syst. Rehabil. Eng.*, vol. 25, no. 10, pp. 1746–1752, 2016.
- [25] Y. Chen, C. Yang, X. Chen, Y. Wang, and X. Gao, “A novel training-free recognition method for SSVEP-based BCIs using dynamic window strategy,” *Journal of neural engineering*, vol. 18, no. 3, p. 036007, 2021.
- [26] K.-R. Müller, M. Krauledat, G. Dornhege, G. Curio, and B. Blankertz, “Machine learning techniques for brain-computer interfaces,” *Biomed. Tech.*, vol. 49, no. 1, pp. 11–22, 2004.
- [27] R. Singla and B. Haseena, “Comparison of ssvep signal classification techniques using svm and ann models for BCI applications,” *International Journal of Information and Electronics Engineering*, vol. 4, no. 1, 2014.
- [28] M. Farooq and O. Dehzangi, “High accuracy wearable SSVEP detection using feature profiling and dimensionality reduction,” in *2017 IEEE 14th International Conference on Wearable and Implantable Body Sensor Networks (BSN)*, pp. 161–164, IEEE, 2017.
- [29] I. A. Ansari, R. Singla, and M. Singh, “SSVEP and ANN based optimal speller design for brain computer interface,” *Computational Science and Techniques*, vol. 2, no. 2, pp. 338–349, 2015.
- [30] T.-H. Nguyen and W.-Y. Chung, “A single-channel SSVEP-based BCI speller using deep learning,” *IEEE Access*, vol. 7, pp. 1752–1763, 2018.
- [31] J. J. Podmore, T. P. Breckon, N. K. Aznan, and J. D. Connolly, “On the relative contribution of deep convolutional neural networks for ssvep-based bio-signal decoding in BCI speller applications,” *IEEE Transactions on Neural Systems and Rehabilitation Engineering*, vol. 27, no. 4, pp. 611–618, 2019.
- [32] A. Ravi, N. H. Beni, J. Manuel, and N. Jiang, “Comparing user-dependent and user-independent training of cnn for SSVEP BCI,” *Journal of neural engineering*, vol. 17, no. 2, p. 026028, 2020.
- [33] Y. M. Chi, Y.-T. Wang, Y. Wang, C. Maier, T.-P. Jung, and G. Cauwenberghs, “Dry and noncontact eeg sensors for mobile brain–computer interfaces,” *IEEE Transactions on Neural Systems and Rehabilitation Engineering*, vol. 20, no. 2, pp. 228–235, 2012.
- [34] N. Aznan, S. Bonner, J. D. Connolly, N. A. Moubayed, and T. Breckon, “On the classification of SSVEP-based dry-EEG signals via convolutional neural networks,” *2018 IEEE International Conference on Systems, Man, and Cybernetics (SMC)*, pp. 3726–3731, 2018.
- [35] Y. Wang, T.-P. Jung, *et al.*, “Visual stimulus design for high-rate SSVEP BCI,” *Electronics letters*, vol. 46, no. 15, pp. 1057–1058, 2010.
- [36] X. Wang, T. Cao, B. Wang, F. Wan, P. U. Mak, P. I. Mak, M. I. Vai, and C. Li, “An online ssvep-based chatting system,” in *Proceedings 2011 International Conference on System Science and Engineering*, pp. 536–539, IEEE, 2011.

- [37] P. Sawangjai, S. Hompoonsup, P. Leelaarporn, S. Kongwudhikunakorn, and T. Wilaiprasitporn, "Consumer grade eeg measuring sensors as research tools: A review," *IEEE Sensors Journal*, vol. 20, no. 8, pp. 3996–4024, 2019.
- [38] R. Maskeliunas, R. Damasevicius, I. Martisius, and M. Vasiljevas, "Consumer-grade eeg devices: are they usable for control tasks?," *PeerJ*, vol. 4, p. e1746, 2016.
- [39] M. Van Vliet, A. Robben, N. Chumerin, N. V. Manyakov, A. Combaz, and M. M. Van Hulle, "Designing a brain-computer interface controlled video-game using consumer grade eeg hardware," in *2012 ISSNIP Biosignals and Biorobotics Conference: Biosignals and Robotics for Better and Safer Living (BRC)*, pp. 1–6, IEEE, 2012.
- [40] P. Arpaia, L. Callegaro, A. Cultrera, A. Esposito, and M. Ortolano, "Metrological characterization of consumer-grade equipment for wearable brain-computer interfaces and extended reality," *IEEE Transactions on Instrumentation and Measurement*, pp. 1–1, 2021.
- [41] D. Gholamiangonabadi, N. Kiselov, and K. Grolinger, "Deep neural networks for human activity recognition with wearable sensors: Leave-one-subject-out cross-validation for model selection," *IEEE Access*, vol. 8, pp. 133982–133994, 2020.

**Andrea Apicella** received the M.S. degree in Computer Science and the Ph.D. degree in Mathematics and Computer Science from the University of Naples Federico II, Italy, in 2014 and 2019, respectively. He is currently a Researcher with the Department of Information Technology and Electrical Engineering of University of Naples Federico II. His current research interests include Artificial Intelligence methods and eXplainable Artificial Intelligence (XAI) approaches for explaining the AI system's decisions.

**Pasquale Arpaia** (SM'14) received the M.S. and Ph.D. degrees in electrical engineering from the University of Naples Federico II, Naples, Italy, in 1987 and 1992, respectively. He was an Associate Professor with the University of Sannio, Benevento, Italy. He is currently a Full Professor of instrumentation and measurements with the University of Naples Federico II, and a Team Leader with CERN, Geneva, Switzerland. Prof. Arpaia is also the Head of the Interdepartmental Research Centre in Health Management and Innovation in Healthcare of the University of Naples Federico II. His current research interests include augmented reality, brain computer interfaces, cyber-security, digital instrumentation and measurement techniques, evolutionary diagnostics, and distributed measurement systems.

**Egidio De Benedetto** (M'14, SM'16) received the M.S. degree in materials engineering and the Ph.D. degree in information engineering from the University of Salento, Lecce, Italy, in 2006 and 2010, respectively. He was with the Institute of Microelectronics and Microsystems, National Research Council, Lecce, Italy, from 2010 to 2012. From 2012 through 2019, he was a Research Fellow with the University of Salento (Lecce, Italy). Since 2019, Egidio De Benedetto is an Associate Professor with the Department of Electrical Engineering and Information Technology of the University of Naples Federico II (Italy).

**Nicola Donato** (SM) received the M.S. degree in electronic engineering from the University of Messina, Messina, Italy, and the Ph.D. degree from the University of Palermo, Palermo, Italy. He is currently an Associate Professor of Electrical and Electronic Measurements and the Head of the Laboratories of "Electronics for Sensors and for Systems of Transduction" and "Electrical and Electronic Measurements" with the University of Messina. His current research interests include sensor characterization and modeling, development of measurement systems for sensors, and characterization of electronic devices up to microwave range and down to cryogenic temperatures.

**Luigi Duraccio** received the M.S. degree (cum laude) in electronic engineering from the University of Naples Federico II in 2018. He developed his master thesis at CERN, Geneva, Switzerland, in the field of radiation measurement for electronics. His current research interests include biomedical instrumentation and measurement, electroencephalographic data acquisition and processing, augmented reality, and brain-computer interfaces.

**Salvatore Giugliano** received the M.S. degree (cum laude) in computer science in 2019. He developed his master thesis in neural networks. His current research interests include analysis and interpretation of EEG signals with machine learning techniques, transfer learning on EEG data and eXplainable Artificial Intelligence. He currently collaborates as a consultant and researcher at the *Villa delle Ginestre* clinic in Volla, Italy.

**Roberto Prevete** received the M.Sc. degree in physics and the Ph.D. degree in mathematics and computer science from the Department of Electrical Engineering and Information Technologies (DIETI), University of Naples Federico II, Naples, Italy. He is currently an Assistant Professor of computer science with the DIETI, University of Naples Federico II. His current research interests include computational models of brain mechanisms, machine learning, and artificial neural networks and their applications. His research has been published in international journals, such as *Biological Cybernetics*, *Experimental Brain Research*, *Neurocomputing*, *Neural Networks*, and *Behavioral and Brain Sciences*.